



REVIEW

# Nanostructured thermoelectric materials: Current research and future challenge

Zhi-Gang Chen<sup>a,\*</sup>, Guang Han<sup>a</sup>, Lei Yang<sup>a</sup>, Lina Cheng<sup>a</sup>, Jin Zou<sup>a,b,\*</sup>

<sup>a</sup>Materials Engineering, The University of Queensland, St Lucia, QLD 4072, Australia

<sup>b</sup>Centre for Microscopy and Microanalysis, The University of Queensland, St Lucia, QLD 4072, Australia

Received 18 July 2012; accepted 7 October 2012

Available online 23 December 2012

## KEYWORDS

Nanostructured thermoelectric materials  
Thermoelectrics  
Power generation

**Abstract** The field of thermoelectrics has long been recognized as a potentially transformative power generation technology and the field is now growing steadily due to their ability to convert heat directly into electricity and to develop cost-effective, pollution-free forms of energy conversion. Of various types of thermoelectric materials, nanostructured materials have shown the most promise for commercial use because of their extraordinary thermoelectric performances. This article aims to summarize the present progress of nanostructured thermoelectrics and intends to understand and explain the underpinnings of the innovative breakthroughs in the last decade or so. We believed that recent achievements will augur the possibility for thermoelectric power generation and cooling, and discuss several future directions which could lead to new exciting next generation of nanostructured thermoelectrics.

© 2012 Chinese Materials Research Society. Production and hosting by Elsevier Ltd. All rights reserved.

\*Corresponding authors at: Materials Engineering, The University of Queensland, St Lucia, QLD 4072, Australia

E-mail addresses: [z.chen1@uq.edu.au](mailto:z.chen1@uq.edu.au) (Z.-G. Chen).

[j.zou@uq.edu.au](mailto:j.zou@uq.edu.au) (J. Zou).

Peer review under responsibility of Chinese Materials Research Society.



## 1. Introduction

The world currently faces numerous challenges relating to energy supply and consumption. The global demand for oil is continuing to increase with record high oil prices [1]. On the other hand, there is a growing concern about the effect - of greenhouse gases, especially carbon dioxide, on the environment. All of these issues are driving the demand for obtaining more useful energy use. For example, many new vehicle engines, transmissions, and associated technologies are under development to increase transport vehicle fuel efficiency. However, these technologies are missing one important issue:

much of the energy will still produce unusable heat in the vehicle exhaust or the cooling system. In fact, in internal combustion engines, approximately 40% of the fuel energy is wasted in exhaust gas, 30% is dissipated in the engine coolant, 5% is lost as radiation and friction, and only 25% is useable for vehicle mobility and accessories [2,3]. Current waste energy assessments indicate that the energy equivalent of 46 billion gallons of gasoline is wasted annually from the exhaust pipes of ~200 million light-duty vehicles in the US alone. In addition, far greater waste heat is generated in the end-to-end electrical production losses, which amounts to around two thirds of available energy in power-generating plants and manufacturing industries. In the US manufacturing sector alone, more than 3000 TW of waste heat energy is lost each year, an amount equivalent to more than 1.72 billion barrels of oil [4]. Therefore, the potential of developing high-efficiency thermoelectric materials for waste-heat-recovery systems (such as thermoelectric generator—TEG) is huge.

High-efficiency thermoelectric materials are an important material system for power generation devices that convert waste heat into electrical energy. The conversion of waste heat into electrical energy plays a key role in our current challenge to develop alternative energy technologies to reduce our dependence on fossil fuels and to reduce greenhouse gas emissions. Previously, thermoelectric materials were used primarily in niche applications. With the advent of broader automotive applications and the effort to utilize waste-heat-recovery technologies, thermoelectric devices are becoming more prominent. This is particularly true with current rising cost of fossil fuels, which has helped spawn a programme between the Energy Efficiency and Renewable Energy office of the US Department of Energy and automotive manufacturers to incorporate thermoelectric waste-heat-recovery technology into the design of heavy trucks. However, current available thermoelectric devices are not in common use, partly due to their low efficiency relative to mechanical cycles and engineer challenges related to using thermoelectric devices for general applications [5]. Therefore, the need of developing high-efficiency thermoelectric materials for waste-heat-recovery systems is urgent and will bring vast economic and environmental benefits.

The conversion efficiency of thermoelectric materials is related to a quantity—called the figure of merit ( $ZT$ ) [6], which is defined as follows:

$$ZT = \frac{S^2 \sigma T}{\kappa} = \frac{S^2 T}{\kappa \rho} = \frac{S^2 T}{(\kappa_e + \kappa_l) \rho} \quad (1)$$

where  $S$  is the Seebeck coefficient,  $\sigma$  and  $\kappa$  are the electrical and thermal conductivity, respectively,  $T$  is the absolute temperature,  $\rho$  is the electrical resistivity, and thermal conductivity ( $\kappa$ ) of thermoelectric materials consists of two parts: lattice thermal conductivity ( $\kappa_L$ ) and electronic thermal conductivity ( $\kappa_e$ ).

The thermoelectric efficiency  $\varepsilon$  in power generation mode and the coefficient of performance  $\eta$  in refrigeration mode (heat is pumped from  $T_C$  to  $T_H$ ) of a thermoelectric couple are given respectively by

$$\varepsilon = \frac{T_H - T_C}{T_H} \left[ \frac{(1 + ZT_M)^{1/2} - 1}{(1 + ZT_M)^{1/2} + (T_C/T_H)} \right] \quad (2)$$

and

$$\eta = \frac{T_C[(1 + ZT)^{1/2} - T_H/T_C]}{(T_H - T_C)[(1 + ZT)^{1/2} + 1]} \quad (3)$$

where  $T_H$ ,  $T_C$  and  $T_M$  are the hot-side, cold-side and average temperatures, respectively, and  $\varepsilon_C$  is the Carnot efficiency and can be expressed as

$$\varepsilon_C = \frac{T_H - T_C}{T_H} \quad (4)$$

As a consequence, a significant difference in temperature (large  $\Delta T$ ) is needed to generate sufficient electrical energy. Currently, thermoelectric research has been focussed on the optimization of a variety of conflicting parameters. To maximize the  $ZT$ , and in turn  $\varepsilon$ , of a material, a large  $\alpha$ , high  $\sigma$ ,

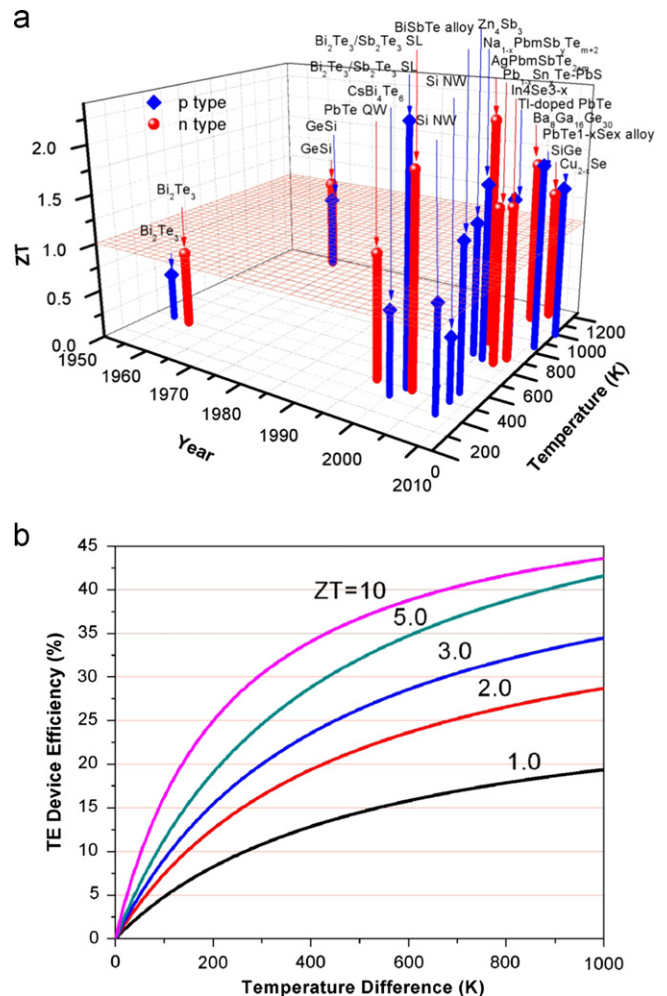


**Fig. 1** (a)  $ZT$  as a function of temperature and year revealing the important development of thermoelectric materials. No material has yet achieved the target goal of  $ZT \geq 3$  to date.  $\text{Bi}_2\text{Te}_3$  [9];  $\text{Bi}_2\text{Te}_3$  [10];  $\text{GeSi}$  [11];  $\text{GeSi}$  [11];  $\text{Pb}_{1-x}\text{Eu}_x\text{Te}/\text{PbTe}$  MQWs [12];  $\text{CsBi}_4\text{Te}_6$  [13];  $\text{Bi}_2\text{Te}_3/\text{Sb}_2\text{Te}_3$  superlattices [14];  $\text{PbSeTe}$ -based QDSL [15];  $\text{AgPb}_m\text{SbTe}_{2+m}$  [16];  $\text{Na}_{1-x}\text{Pb}_m\text{Sb}_y\text{Te}_{m+2}$  [17];  $\text{Ba}_8\text{Ga}_{16}\text{Ge}_{30}$  [18];  $\text{Si}$  NWs [19];  $\text{Si}$  NWs [20];  $\text{BiSbTe}$  bulk alloy [21];  $\beta\text{-Zn}_4\text{Sb}_3$  [22];  $\text{Pb}_{1-x}\text{Sn}_x\text{Te-PbS}$  [23];  $\text{TI}$ -doped  $\text{PbTe}$  [24];  $\text{SiGe}$  [25];  $\text{In}_4\text{Se}_{3-\delta}$  [26];  $\text{Na}$ -doped  $\text{PbTe}_{1-x}\text{Se}_x$  alloy [27];  $\beta\text{-Cu}_{2-x}\text{Se}$  bulk material [28]; (b) Thermoelectric energy conversion as a function of  $ZT$  at the setting of  $T_c = 300$  K.

and low  $\kappa$  are required [7,8]. The requested fine integrated measuring system allows these key parameters to be accurately measured. While there is no theoretical limit for the maximum ZT, the best bulk thermoelectric materials found so far, such as  $\text{Bi}_2\text{Te}_3$ ,  $\text{PbTe}$ , and  $\text{Si}_{1-x}\text{Ge}_x$ , have shown a maximum ZT value about 1, which restricts the large-scale application of thermoelectric technology. A few remarkable progresses have been made to improve the thermoelectric properties, especially recent achievements to create nanostructured materials, such as superlattices, quantum dots, nanowires, and nanocomposite, as shown as plots in Fig. 1a, which indicate that major milestones achieved for ZT over the past several decades as a function of both year and temperature.

Despite such a high anticipation and achievements, the progress in the thermoelectric materials has still been limited to those current thermoelectric materials for practical applications. The commercial thermoelectric materials have a relative low ZT of 1 and the average thermoelectric generators on the market have a conversion efficiency of approximately 5%, as shown in Fig. 1b. As can be seen, there is a great potential to seek new materials with ZT values of 2–3 to provide the desired conversion efficiencies to be competitive with traditional mechanical energy conversion systems. For a typical example, a thermoelectric power conversion device with ZT=3 operating between 773 and 303 K (room temperature) would yield ~50% of the Carnot efficiency [29]. Therefore, it is critical to synthesize thermoelectric materials with high ZT in order to promote the practical applications of thermoelectric materials.

The major activities in thermoelectric materials have been focussed on the increase of the Seebeck coefficient and the reduction of the thermal conductivity. Several key reviews have been surveyed on developments in bulk materials [30], nanoscale [31–33], or bulk nanostructured thermoelectric materials [1,6,34], whilst progress in understanding the key feature of the influence of interfaces on thermoelectric performance [35] and theory on nanostructured thermoelectric [36,37] has also been comprehensively reviewed. Here, this review tries to highlight the significant progress in the past several years and understand the enhanced thermoelectric properties of nanostructured or nanoscale materials. The organization of the review is as follows. First, we discuss the basic principles for improving thermoelectric performance along with the basic methodology. And then we highlight the current research progress and focus on addressing nanostructured thermoelectric materials with ZT over 1. Finally, we identify strategies and research directions which could lead to the next generation of nanostructured thermoelectric materials.

## 2. Basic theory and methodology for improving ZT

A material with high ZT needs to have a large Seebeck coefficient, existed in low carrier concentration semiconductors or insulators, and a high electrical conductivity, found in high carrier concentration metals; therefore, the thermoelectric power factor maximizes somewhere between the carrier concentrations of semiconductors and metals, as revealed in Fig. 2 [32]. Specifically, the relationship between the Seebeck coefficient and carrier concentration can be expressed as

$$S = \frac{8\pi^2 k_B^2}{3eh^2} m^* T \left( \frac{\pi}{3n} \right)^{2/3} \quad (5)$$

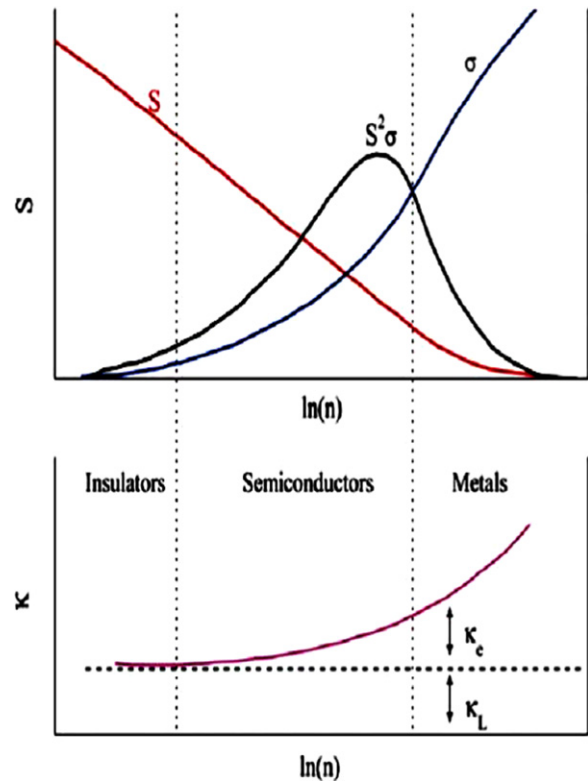


**Fig. 2** Illustration of the variation of the Seebeck coefficient ( $S$ ), electrical conductivity ( $\sigma$ ), power factor ( $S^2\sigma$ ), electronic thermal conductivity ( $\kappa_e$ ), and lattice ( $\kappa_L$ ) thermal conductivity on the charge carrier concentration  $n$ , for a bulk material. Reproduced from Ref. [38].

where  $k_B$  is the Boltzmann constant,  $e$  is the carrier charge,  $h$  is Planck's constant,  $m^*$  is the effective mass of the charge carrier, and  $n$  is the carrier concentration. The relationship between electrical conductivity and carrier concentration can be defined as

$$\sigma = ne\mu \quad (6)$$

where  $\mu$  is the carrier mobility. Typically, good thermoelectric materials are heavily doped semiconductors with carrier concentration of  $10^{19}$ – $10^{21} \text{ cm}^{-3}$  [32]. To ensure the Seebeck coefficient is large, a single type of carriers (n-type or p-type) should be remained, as mixed n-type/p-type charge carriers will lead to the opposite Seebeck effect and hence low thermopower. In order to achieve single type of carriers, it is necessary to select materials with suitable energy bandgaps and appropriate doping, in which n-type and p-type can be well separated. Therefore, effective thermoelectric materials are heavily doped semiconductors with energy bandgap less than 1 eV, in order to have both a single carrier type and sufficiently high carrier mobility. It is evident that decoupling the thermal and electronic terms that determine the ZT, including the Seebeck coefficient and electrical conductivity, has been a key strategy to improve ZT.

An effective thermoelectric material also needs to have a low thermal conductivity. Thermal conductivity of thermoelectric materials consists of two parts:  $\kappa_L$ , which results from heat transporting phonons travelling through the crystal lattice, and  $\kappa_e$ , which arises from heat carrying charge carries (electrons or

holes) moving through the crystal lattice. According to the Wiedemann–Franz Law

$$\kappa_e = L\sigma T \quad (7)$$

where  $L$  is the Lorenz number, the electronic thermal conductivity is proportional to the electrical conductivity, as shown in Fig. 2. Therefore, to reduce the electronic component of the thermal conductivity for thermoelectric materials is not always best choice, since it will inversely affect the electrical conductivity and has little or no improvement of ZT. Lattice thermal conductivity can be defined by

$$\kappa_l = 1/3(C_v v_s \lambda_{ph}) \quad (8)$$

where  $C_v$  is heat capacity,  $v_s$  is the sound velocity, and  $\lambda_{ph}$  is the phonon mean free path (mfp). It can be seen that lattice thermal conductivity is the only parameter not determined by the electronic structure, so that enhancement of ZT can be achieved by minimizing the lattice thermal conductivity.

There are two primary methodologies in searching for thermoelectric materials with high ZT. The first approach is the “phonon glass electron crystal” (PGEC) approach, which suggests that an ideal thermoelectric material should be the combination of glass-like thermal conductivity and crystal-like electronic properties [39]. This approach is the most achievable in materials with complex crystal structures, where voids (vacancies) and rattlers (heavy element atoms located in the voids) would act as effective phonon scattering centres and reduce the lattice thermal conductivity significantly. The other approach is the nanostructuring of thermoelectric materials, which suggests that the ZT enhancement can be realized with nanoscale or nanostructured morphologies [33,40,41]. Nanostructuring can enhance the density of states (DOS) near Fermi level via quantum confinement and therefore increase the thermopower, which provides a way to decouple thermopower and electrical conductivity [33,40,41]. Besides, because mfp of electrons is much shorter than that of photons in heavily doped semiconductors, nanostructuring serves to introduce a large density of interfaces in which phonons over a large mfp range can be scattered more effectively and preferentially than electrons, as illustrated in Fig. 3, hence reducing the lattice thermal conductivity effectively while preserving carrier mobility and electronic conduction [40]. This can be satisfied

by preparation of nanostructures with one or more dimensions smaller than the mfp of phonons, while still larger than that of charge carriers.

### 3. Research progress on thermoelectric materials

As shown in Fig. 1a, the field of thermoelectrics advanced rapidly in the 1950s where scientific basis of thermoelectric materials became well established. The first generation of thermoelectric materials, such as  $\text{Bi}_2\text{Te}_3$ ,  $\text{PbTe}$  and  $\text{SiGe}$  bulk thermoelectric materials, were developed for applications at room temperature, intermediate temperature and high temperature, respectively. In the 1960s, the leading method for improving ZT was to control doping and form solid solutions, such as  $\text{Bi}_2\text{Te}_3\text{--Sb}_2\text{Te}_3$ ,  $\text{PbTe--SnTe}$ , and  $\text{Si}_{1-x}\text{Ge}_x$ . Although point defects in solid solutions serve to decrease the lattice thermal conductivity by increasing heat carrying phonons scattering, there were also concurrent reductions in the charge carrier mobility, therefore, the overall ZT enhancement is limited [33]. From 1960 to 1990, the field of thermoelectrics received little attention globally, in which  $(\text{Bi}_{1-x}\text{Sb}_x)_2(\text{Se}_{1-y}\text{Te}_y)_3$  alloy family remained the best commercial material with ZT of about 1 [41]. In 1990s, thermoelectric community is encouraged to re-investigate advanced thermoelectric materials with high performance for thermoelectric power generation and cooling applications. For this reason, there is a revival of interest in the development of high-performance thermoelectric materials and the relevant thermoelectric theory. Over the past two decades, two different approaches have been developed to search for the next generation of thermoelectric materials: one is finding and using new families of bulk thermoelectric materials with complex crystal structures, and the other is synthesizing and using low-dimensional thermoelectric materials systems. Significant ZT improvement has been reported in the PGEC materials, and nanostructured materials, such as superlattices, quantum dots, nanowires, and nanocomposite. The key breakthroughs are highlighted in Fig. 1a. Here, we will briefly mention the progress on PGEC materials and highlight the progress on nanostructured thermoelectric materials

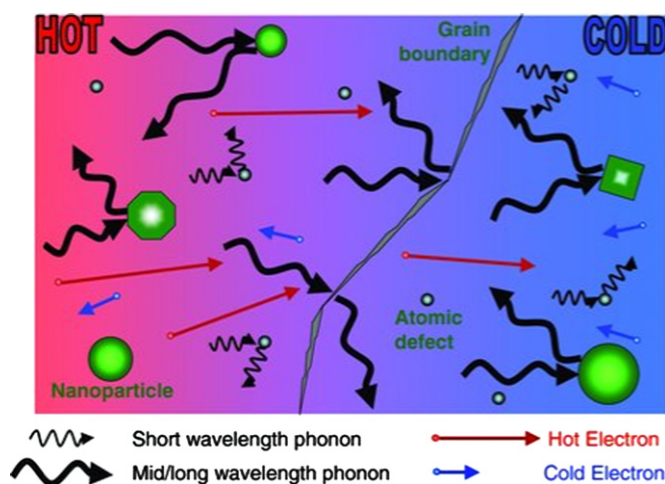


Fig. 3 Schematic diagram illustrating phonon scattering mechanisms and electronic transport of hot and cold electrons within a thermoelectric material. Reproduced from Ref. [31].



### 3.1. PGEC thermoelectric materials

Slack [39] suggested that the best thermoelectric materials would behave as “phonon glass electron crystal”, that is, it would have the thermal properties of glass-like materials and the electrical properties of crystalline materials. In typical PGEC materials, high mobility electrons are able to transport charge and heat freely, while the phonons are disrupted at the atomic scale from transporting heat. Generally, these materials contain a large amount of large interstitial sites filled with other element atoms, which act as “rattler” atoms that vibrate at low frequencies and consume thermal energy. Therefore, the PGEC materials act like a crystal for electrons while still efficiently scatter phonons, rendering these materials retaining high electrical conductivities and also obtaining low thermal conductivities. Typical examples of PGEC thermoelectric materials are skutterudites [42–52], clathrates [53–62] and  $\beta$ -Zn<sub>4</sub>Sb<sub>3</sub> [22,63,64].

CoSb<sub>3</sub> is a typical skutterudite compound, which crystal structure is illustrated in Fig. 4a. Its crystal structure belongs to body-centred cubic with eight CoSb<sub>3</sub> formula units, which can be regarded as a simple cubic transition metal Co sublattice partially filled by almost square ring Sb<sub>4</sub>. These rings fill six out of eight cubes formed by Co atoms, while the remaining two cubes (voids) are empty and can be filled by other atoms as “rattlers”. The original CoSb<sub>3</sub> has a very high power factor, but its lattice thermal conductivity is too high to be an effective thermoelectric material. One successful approach for improving ZT of these materials is proved to be void-filling in the structure with many different elements, including lanthanide, actinide, alkaline-earth, alkali, and Group IV elements [30]. These atoms can act as effective

phonon scattering centres to substantially reduce the lattice thermal conductivity. Smaller and heavier atoms in the voids would result in larger disorder and lead to larger reduction of the lattice thermal conductivity.

$ZT \geq 1$  has been achieved in filled skutterudites [42–52]. For example, Ba<sub>0.08</sub>La<sub>0.05</sub>Yb<sub>0.04</sub>Co<sub>4</sub>Sb<sub>12</sub> has achieved a ZT of 1.7 at 850 K, which is the highest ZT value for the skutterudites as shown in Fig. 4c [52]. The clathrates are low-thermal conductivity compounds with open frameworks composed of tetrahedrally coordinate Si, Ge, Al, Ga, or Sn. The framework has cages that can incorporate large electropositive atoms. There are two main types of structure, so-called Type I and Type II, with the former being more common. The typical structure is shown in Fig. 4b. Recent research for optimizing the thermoelectric properties of Type I clathrates above room temperature showed promising results, as shown in Fig. 4d. A Ba<sub>8</sub>Ga<sub>16</sub>Ge<sub>30</sub> crystalline ingot showed a Seebeck coefficient of –45 to –150 mV K<sup>-1</sup> and electrical conductivity 1500–600 Scm<sup>-1</sup> at 300–900 K [18]. The thermal conductivity of this sample decreased from 1.8 W m<sup>-1</sup> K<sup>-1</sup> at 300 K to 1.25 W m<sup>-1</sup> K<sup>-1</sup> at 900 K, which gave rise to ZT of 1.35 [18].

### 3.2. Nanostructured thermoelectric materials

Low-dimensional thermoelectric materials are believed to have higher thermoelectric properties than their bulk counterparts, because the DOS near Fermi level can be enhanced via quantum confinement therefore leading to the increase of thermopower; and/or because phonons over a large mfp range can be effectively scattered by high density of interfaces, hence resulting in the decrease of the lattice thermal conductivity. Significant ZT

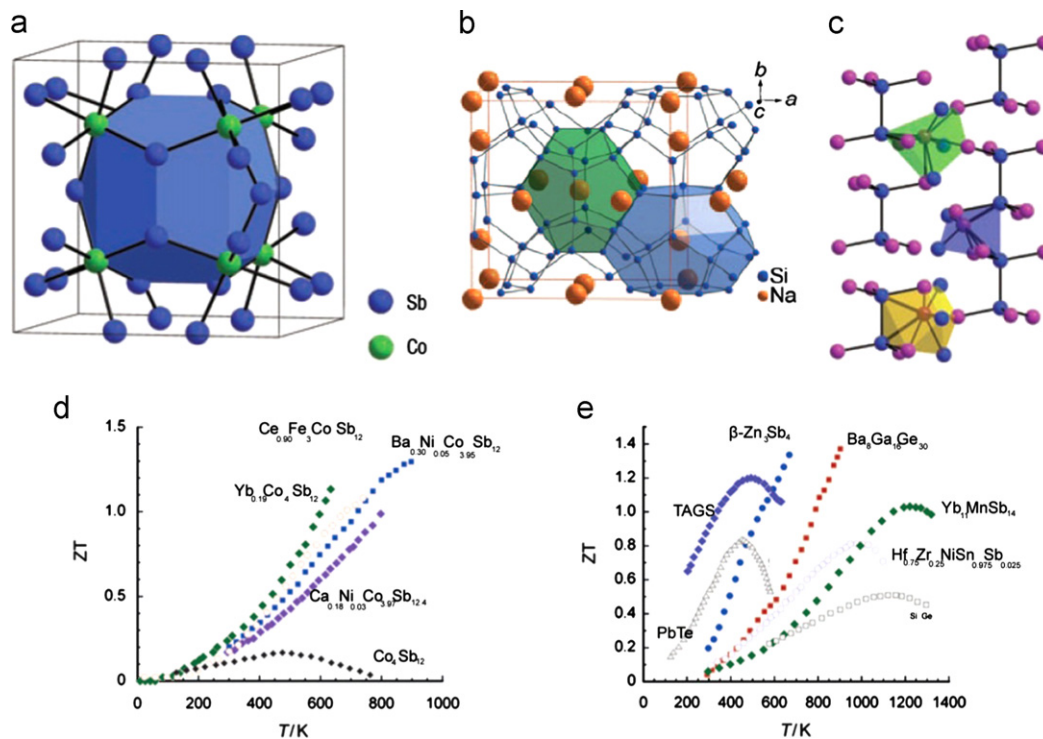


**Fig. 4** (a–c) Crystal structure of CoSb<sub>3</sub> revealing the large voids with rattlers (rattlers), the type I clathrate Na<sub>8</sub>Si<sub>46</sub>, and  $\beta$ -Zn<sub>4</sub>Sb<sub>3</sub>, reproduced from Ref. [63]; (d) ZT as a function of temperature for skutterudites as thermoelectric materials (e) Variable temperature ZT of clathrates, and  $\beta$ -Zn<sub>4</sub>Sb<sub>3</sub>, reproduced from Ref. [30].

enhancement has been found in two-dimensional (2D) and one-dimensional (1D) thermoelectric materials.

### 3.2.1. 2D thermoelectric nanomaterials: quantum wells and superlattices

Kicks and Dresselhaus [65] pioneered improved ZT by two-dimensional  $\text{Bi}_2\text{Te}_3$  quantum well due to the enhancement of thermopower, as quantum confinement in the interlayer direction can increase the DOS near the Fermi level. They also suggested that the interfaces between layers would effectively scatter phonons if the  $\text{Bi}_2\text{Te}_3$  layer thickness was less than phonon mfp, which would result in the decrease of lattice thermal conductivity [65,66]. As revealed in Fig. 5, the ZT of  $\text{Bi}_2\text{Te}_3$  quantum well structures are projected to be much higher than its bulk counterparts. Venkatasubramanian et al. [14] observed the highest  $\text{ZT}=2.4$  using  $\text{Bi}_2\text{Te}_3\text{-Sb}_2\text{Te}_3$  quantum well superlattices with a periodicity of 6 nm. Correspondingly, the highest ZT value for the bulk counterparts is only  $\text{ZT}=1.1$ . Inspired by the prediction that quantum confinement may lead to an increased Seebeck coefficient and therefore higher ZT, Harman and coworkers [15] developed quantum-dot superlattices in the  $\text{PbTe-PbSeTe}$  system, described as  $\text{PbSe}$  nanodots embedded in a  $\text{PbTe}$  matrix, and showed  $\text{ZT}=1.6$ , which is significantly higher than their bulk counterparts ( $\text{ZT}=0.34$ ). Enhanced thermoelectric properties have also been found in two-dimensional thin films and quantum well structures, including  $\text{Bi}_2\text{Te}_3$  superlattice-based thin-film [67],  $\text{PbTe/Ag}_2\text{Te}$  thin films [68], quantum well/barrier  $\text{PbTe/Pb}_{1-x}\text{Eu}_x\text{Te}$  structures [69], and  $n\text{-PbTe/p-SnTe/n-PbTe}$  quantum wells [70]. The early motivation for these investigations was based on the prediction that quantum confinement of in-plane carrier transport could substantially enhance the power factor over that of homogeneous materials, leading to ten-fold increases in ZT [65]. Shakouri [71] considered that such enhancement could occur because sharp features in the electronic density of states of quantum-confined structures enable a doping-level-tuneable increase in the asymmetry between hot and cold electron transport, resulting in a large average transport energy and a large number of carriers moving in the material (i.e., a large Seebeck coefficient and electrical conductivity) [31].

Devices based on two-dimensional thermoelectric materials (such as thin film, quantum well, and superlattices) may be used for small-scale electronic and optoelectronics applications where small heat loads or low levels of power generation are required [67]. However, their thermal and chemical stability associated with thermo- and electro-migration are of great concern. Especially, fully functional practical thermoelectric coolers have not been made from these nanomaterials due to the enormous difficulties in integrating nanoscale materials into microscale devices and packaged macroscale systems.

### 3.2.2. 1D thermoelectric nanomaterials: nanowires

Theoretical studies predict a large enhancement of ZT inside quantum wires due to additional electron confinement. Quantum nanowires were suggested to have greater enhancement in thermoelectric performance due to their stronger quantum confinement and phonon scattering, in comparison to two-dimensional counterparts [72]. It has also been proposed that nanotubes may have lower lattice thermal conductivity than nanowires due to their

additional phonon scattering on the inner and outer surfaces of nanotubes [73,74]. Up to date, there have been many reports on the enhancement of thermoelectric properties in one-dimensional materials. Hochbaum et al. [20] reported  $\text{ZT}=0.6$  can be obtained at room temperature for 50 nm diameter silicon nanowires with rough surfaces synthesized by electroless etching, which represents a 60-fold increase in ZT compared to its bulk counterpart, because the rough nanowire surface could scatter phonons effectively. The thermal conductivity, power factor and ZT of the nanowires are shown in Fig. 6. Boukai et al. [19] found that thermal conductivity decreases with decreasing the nanowire diameter, and reported a ZT of 1 at 200 K for nanowires with 20 nm diameter, resulting from the significant decrease of thermal conductivity and an enhanced phonon drag contribution to the thermopower. This is the first claim that phonon drag can enhance ZT significantly in rough nanowires. Boukai et al. [19] believed that the Seebeck coefficient can be increased by the transport of certain phonon modes which have minimal contribution to thermal conductivity. It also has been reported that some nanowires have equal or lower thermoelectric properties compared to their bulk materials [75,76], which may be due to the limited ability to control dopant and impurity concentrations in nanowires [76,77], and unintentional doping resulting from surface oxidation [78].

Thermoelectric measurements on individual building block, such as nanotubes, nanowires, and nanobelts, have been achieved using a suspended microheater platform [79]. However, in many practical energy conversion applications, nanowire arrays are required and the whole structure should be embedded in a matrix. A potential p-n heterostructure array used as building block to assemble thermoelectric device is proposed for potential module, as shown in the model of Fig. 7. The challenge in ensuring good electrical contact to all nanowires in the array, having high packing densities and minimizing matrix heat leakage is preventing measuring any significant enhancement in nanowire composites [31].

### 3.2.3. Nanocomposites

Nanostructured thermoelectric materials are designed to introduce nanometer-sized polycrystallines and interfaces into

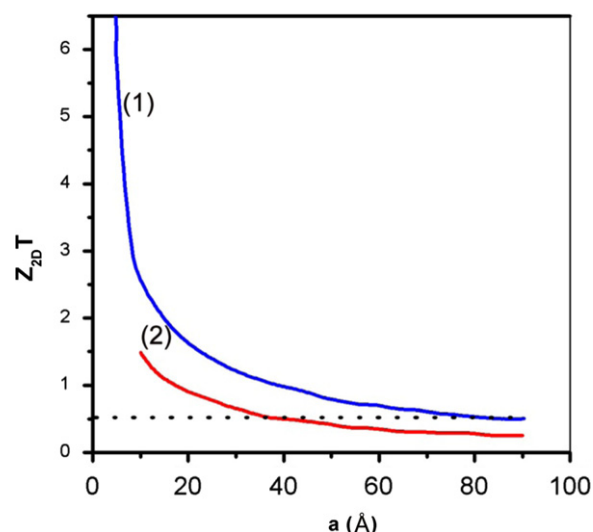
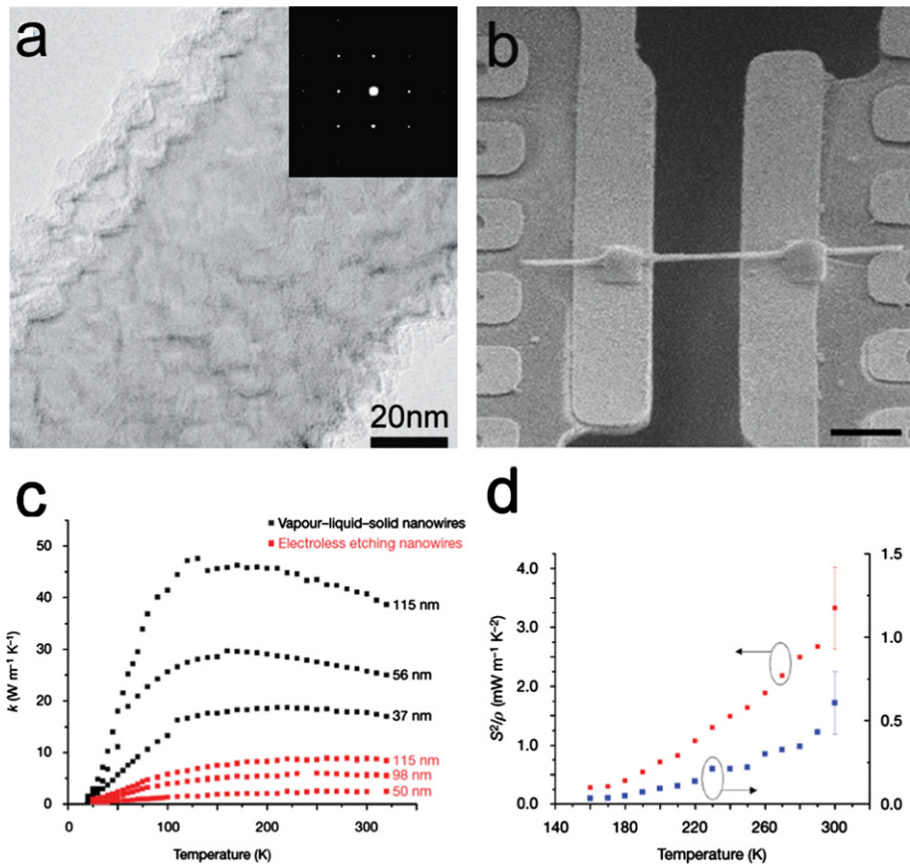
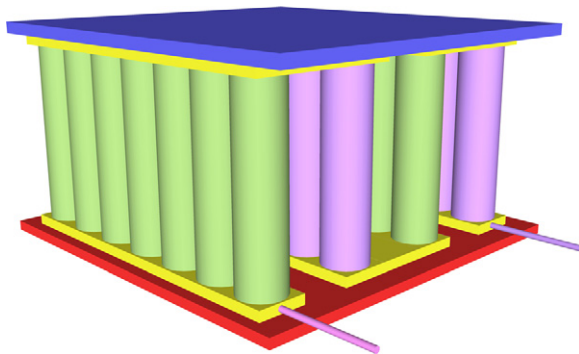


Fig. 5 Calculated ZT as a function of layer thickness  $a$  in a quantum well structure for layers parallel to the  $a$ - $b$  plane (1) and  $b$ - $c$  plane (2), and the dashed line represents the optimized ZT for bulk  $\text{Bi}_2\text{Te}_3$ . Reproduced from Ref. [65].



**Fig. 6** (a) Typical microstructure of rough Silicon nanowires by electroless etching; (b) Devices assembly; (c) The thermal conductivity  $\kappa$ ; and (d) Power factor and ZT of nanowires synthesized by electroless etching. Reproduced from Ref. [20].



**Fig. 7** p-n junction heterostructure array-based thermoelectric modulus.

bulk materials, which can reduce the lattice thermal conductivity by increasing the phonon scattering. Preferential phonon scattering is possible, as the phonon mfp typically ranges from several nanometres up to a few hundred nanometres, while the carrier mfp is typically only a few nanometres [40]. Therefore, incorporation of nanostructures covering various length scales can reduce the lifetime of phonons with a broad mfp distribution, while charge transport can remain unchanged [40]. The approach to achieve nanostructuring composites through the formation of nanometer-sized (grain size  $\sim 5$  nm–10  $\mu$ m) polycrystallines, typically fabricated by hot pressing or spark plasma sintering of fine powders formed by grinding and milling or wet chemistry processing, in which thermoelectric

materials are prepared in nanosized particles and are then hot pressed into monoliths. Such an approach creates extensive interfaces between the neighbouring nanoparticles, which can significantly lower the thermal conductivity. The resulting nanocomposites can exhibit several benefits over conventional techniques that create very large-grain or single crystal material, such as reduced thermal conductivity (due to phonon scattering at grain boundaries, as illustrated in Fig. 3), increased power factor (due to electron filtering at grain boundaries), better mechanical properties and improved isotropy [31]. Compacting nanocrystalline samples can be a relatively low-cost method to provide the large volume of material necessary for more wide-spread adoption of thermoelectric technology. ZT enhancement has been found in the many kinds of nanostructured material families, including  $\text{Bi}_2\text{Te}_3$ -based nanocomposites [21,80–89],  $\text{PbTe}$ -based nanostructured materials [16,17,23,34,90–106], and  $\text{SiGe}$ -based nanocomposites [25,107].

**3.2.3.1.  $\text{Bi}_2\text{Te}_3$ -based nanocomposites.**  $\text{Bi}_2\text{Te}_3$  and their related nanocomposites, the best thermoelectric materials at room temperature, are extensively used for the first thermoelectric devices for commercial Peltier elements.  $\text{Bi}_2\text{Te}_3$  crystals belong to the rhombohedral crystal system with a layer structure, as shown in Fig. 8. Each layer is composed of a Te–Bi–Te–Bi–Te unit, and each unit cell is composed of an ABC stacking of Te–Bi–Te–Bi–Te units along its  $c$ -axis direction. The layers are connected by the van der Waals force, while within the layer, both covalent and ionic bonds are dominated. Therefore, the



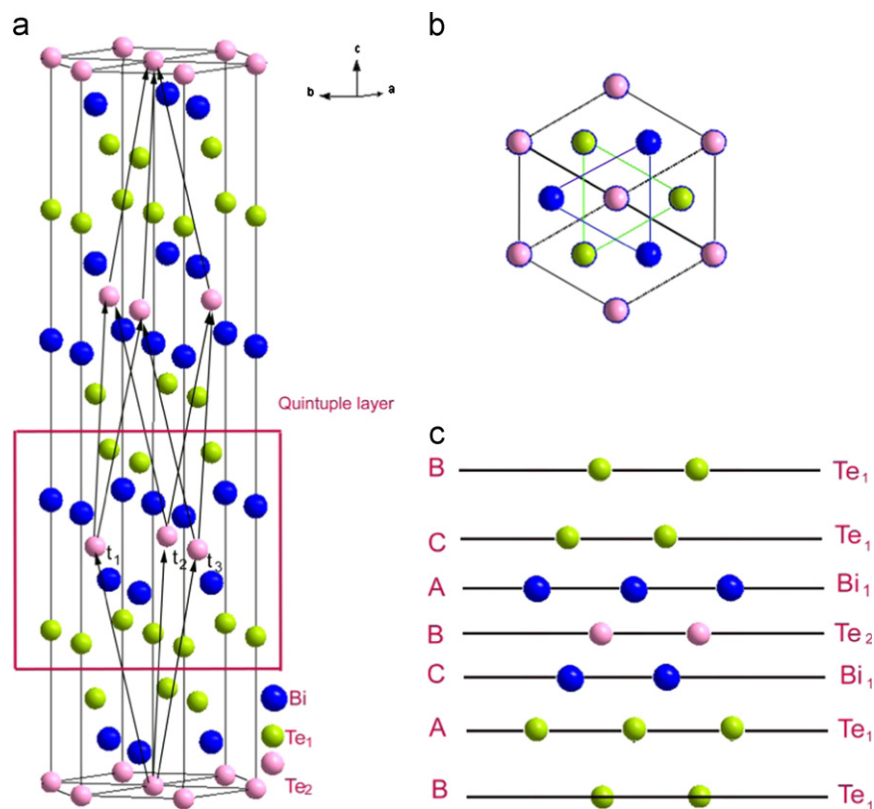


**Fig. 8** Crystal structure of  $\text{Bi}_2\text{Te}_3$ . (a) Crystal structure of  $\text{Bi}_2\text{Te}_3$  with three primitive lattice vectors denoted as  $t_{1,2,3}$ . A quintuple layer with  $\text{Te}_1\text{-Bi}_1\text{-Te}_2\text{-Bi}_1\text{-Te}_1$  is indicated by the red square; (b) Top view along the  $z$ -direction. The triangle lattice in one quintuple layer has three different positions; (c) Side view of the quintuple layer structure.

interlayer interactions are much weaker than the intra-layer interaction.

A polycrystalline p-type  $\text{Bi}_{0.5}\text{Sb}_{1.5}\text{Te}_3$  bulk nanocomposite (as shown in Fig. 9), fabricated by hot pressing of ball-milled nanopowders, exhibited ZT of 1.2 at room temperature and ZT of 1.4 at 373 K [21]. The thermal conductivity was significantly reduced to  $1.0 \text{ W m}^{-1} \text{ K}^{-1}$  in the nanocomposite from  $1.3 \text{ W m}^{-1} \text{ K}^{-1}$  in the bulk ingots of the same material, although the electrical conductivity was slightly reduced in the nanocomposite; therefore, the maximum ZT of the nanocomposite was almost 30% higher than the bulk ingots. Transmission electron microscopy characterization of this nanocomposite is revealed in Fig. 9a–c. Complex polygonal grain structures, with diameters ranging from a few microns down to a few nanometres were detected in the nanocomposite. In addition, Sb-rich nanodots ranging from 2 to 10 nm in diameter with diffuse boundaries and pure Te precipitates with diameter between 5 and 30 nm were also observed. These nanostructures could effectively scatter phonons with a broad wavelength, which may account for the enhancement of thermoelectric properties in the nanostructured  $\text{Bi}_2\text{Te}_3$ -based nanocomposites. Their following research further show other p-type  $\text{Bi}_2\text{Te}_3$ -based nanocomposites can also achieve a high ZT, about 1.3 between 75 and 373 K [80] and 1.4 at 373 K [81], and synthesized n-type  $\text{Bi}_2\text{Te}_3$ -based nanocomposite with a ZT of 1.04 at 398 K [82].

In the reports on properties of  $\text{Bi}_2\text{Te}_3$ -based nanocomposites, there exists a wide variation in ZT values, ranging from  $\sim 0.4$  to 1.7 for nanocomposites with similar compositions. For example, a high ZT of about 1.5 at 390 K was achieved in

$(\text{Bi,Sb})_2\text{Te}_3$  nanocomposites by melt spinning single elements of Bi, Sb, and Te followed by the spark plasma sintering process.  $\text{ZT} = 1.47$  [84] and  $\text{ZT} = 1.56$  [85,86] were achieved in nanocomposites fabricated by hot pressing of  $\text{Bi}_2\text{Te}_3$  and  $\text{Sb}_2\text{Te}_3$  nanopowders with diameters below 20 nm and p-type  $\text{Bi}_{0.52}\text{Sb}_{1.48}\text{Te}_3$  with 5–15 nm diameter precipitates produced by melt spinning and spark plasma sintering. Other  $\text{Bi}_2\text{Te}_3$ -based nanocomposites have revealed similar thermoelectric properties to bulk  $\text{Bi}_2\text{Te}_3$  [73,88], while some others have poor performance in contrast [89]. It can be deduced that the detailed structural and compositional characteristics of the nanostructures should play an important role in the thermoelectric performance.

**3.2.3.2. PbTe-based nanostructured materials.** A very high ZT of about 2.2 was achieved in complex nanostructured PbTe-based alloy  $\text{Ag}_{1-x}\text{Pb}_{18}\text{SbTe}_{20}$  (LAST) fabricated by the melt-grown method [16]. TEM analysis suggests that the LAST alloys are complex nanostructured composites containing Ag–Sb-rich nanoscale inclusions, as revealed in Fig. 10, particularly when deviations from the ideal stoichiometry can be detected [16]. These nanoscale inclusions played an important role in reducing the thermal conductivity, which lead to a thermal conductivity of about  $2.3 \text{ W/m K}$  at room temperature. A number of other PbTe-based nanostructured materials, including  $\text{AgPb}_m\text{SbTe}_{2+m}$  (LAST-m),  $\text{AgPb}_m\text{Sn}_n\text{SbTe}_{2+m+n}$  (LASTT),  $\text{NaPb}_m\text{SbTe}_{2+m}$  (SALT-m),  $\text{KPb}_m\text{SbTe}_{m+2}$  (PLAT-m) and PbTe–PbS, have also achieved ZT values high than 1 [17,23,90–105].  $\text{AgPb}_m\text{SbTe}_{m+2}$  fabricated by combining



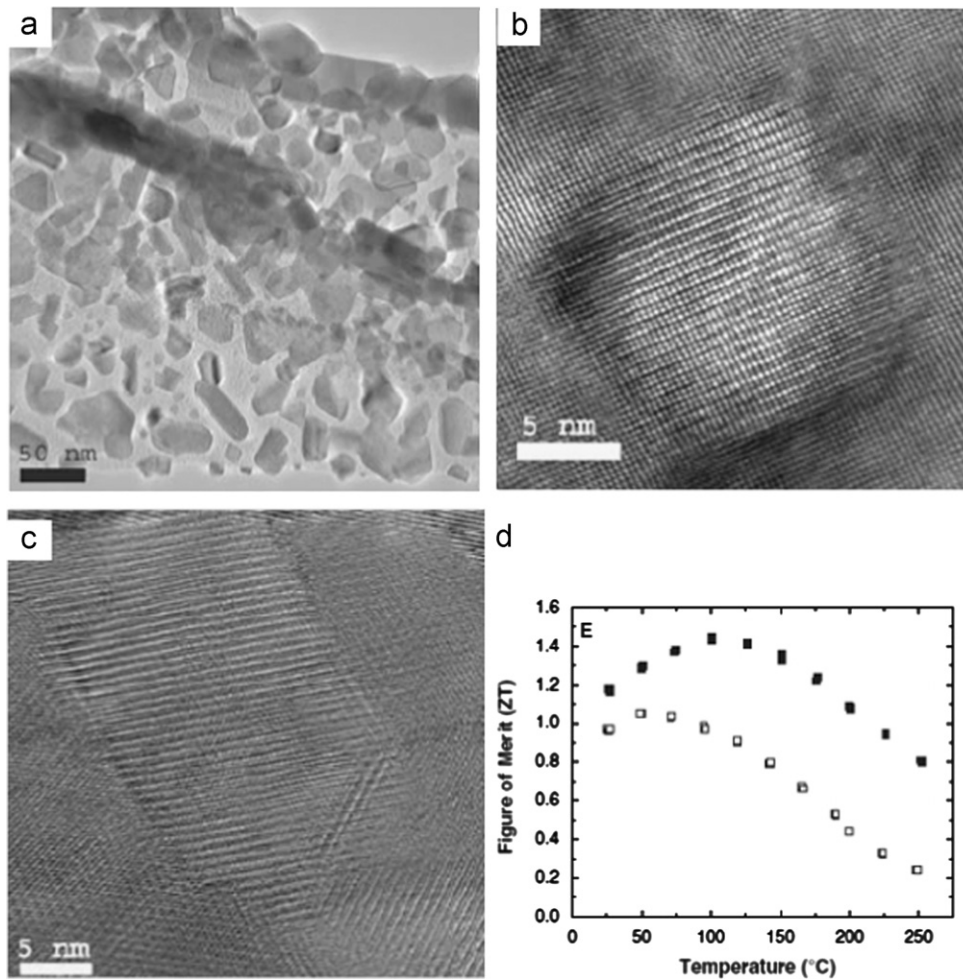


**Fig. 9** TEM images showing the microstructures of a hot-pressed  $\text{Bi}_x\text{Sb}_{2-x}\text{Te}_3$  nanocomposite and their thermoelectric performance. (a) Nanosized grains with clear grain boundaries. (b) High-magnification image showing the nanosize, high crystallinity, random orientation, and clean grain boundaries. (c) Nanodot without grain boundaries. (d) ZT. Reproduced from Ref. [21].

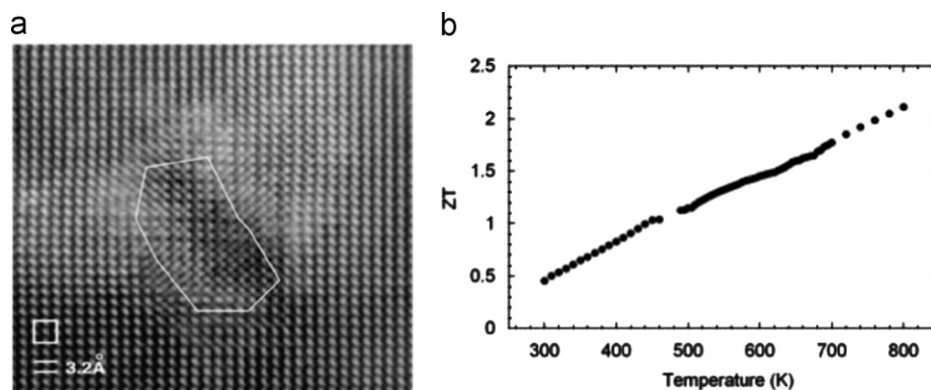


**Fig. 10** (a) TEM image of a  $\text{AgPb}_{18}\text{SbTe}_{20}$  sample showing a nanosized region (a “nanodot” shown in the enclosed area) of the crystal structure that is Ag-Sb-rich in composition; (b) ZT. Reproduced from Ref. [16].

mechanical alloying and spark plasma sintering methods can also achieve a high ZT of 1.5 at 700 K [106].

**3.2.3.3. SiGe-based nanocomposites.** A significant improvement in ZT was achieved in p-type SiGe nanocomposites, with a peak value about 0.95 at 1173–1223 K through a ball milling and hot-pressing method [107]. The ZT improvement

was about 90% over that of radioisotope thermoelectric generator samples (peak  $\text{ZT}=0.5$ ), and 50% over the previous highest record (0.65) [108]. A peak ZT of  $\sim 1.3$  at 1173 K was also achieved in n-type SiGe nanocomposites using the ball milling and hot-pressing method [25], as shown in Fig. 11. Boron-doped Si/Ge nanocomposites formed by ball milling and hot pressing were also reported to significantly reduce thermal

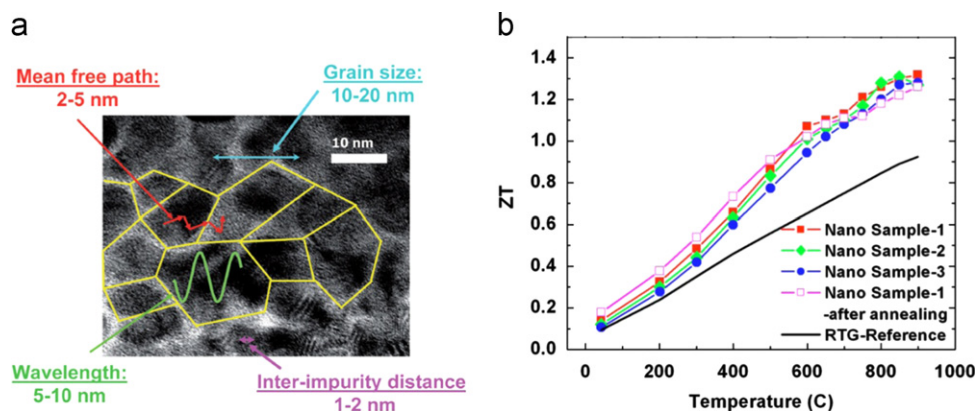


**Fig. 11** (a) A TEM image of a heavily doped  $\text{Si}_{80}\text{Ge}_{20}$  nanocomposite along with some important numerically calculated characteristic lengths [6], and (b) typical ZT. Reproduced from Ref. [25].

conductivities compared to bulk SiGe alloys [41]. In addition, such SiGe nanocomposites had increased Seebeck coefficients and only slightly reduced electrical conductivities, resulting in somewhat higher power factors over the temperature range of 300–1000 K. This increased power factor for the nanocomposite is much similar to what was observed for the  $\text{Bi}_x\text{Sb}_{2-x}\text{Te}_3$  alloy and predicted based on electron filtering effects at the grain boundaries.

The materials used in thermoelectric power generation and cooling applications in the near future are nanostructured nanocomposite thermoelectric materials, as they can be assembled into a variety of desired shapes for device applications, and can be scaled up for commercial applications. These nanocomposites have already revealed dramatic improvements in thermoelectric efficiency over their bulk counterparts, and many can be fabricated through relatively inexpensive processing techniques. It should be noted that the details of the nanostructures (grain size, morphology, and compositions) and the preparation conditions must have a large impact on the performance of nanocomposite thermoelectric materials, and continued research to obtain a deeper understanding is required to allow the rational design and preparation of nanocomposites and accelerate the wide adoption of thermoelectric technologies in power generation and cooling applications.

As summarized in Table 1, reducing the size and dimensionality of thermoelectric materials in nanoscale and nanostructured materials has been demonstrated to be one of the best methods to increase the thermoelectric performance, which confirmed the predicted ZT enhancement due to quantum confinement and nanostructure effects [65]. These increased ZT values result primarily from lowered thermal conductivity as interface density increases, as well as from possible quantum size effects including improved thermopower resulting from the increased electronic DOS at the Fermi level in low-dimensional systems [40]. From Table 1, a record apparent highest ZT of 2.4 was reported for the  $\text{Bi}_2\text{Te}_3/\text{Sb}_2\text{Te}_3$  superlattice system [14] and a remarkably low 300-K cross-plane value of  $0.22 \text{ W m}^{-1} \text{ K}^{-1}$  was estimated in this  $\text{Bi}_2\text{Te}_3/\text{Sb}_2\text{Te}_3$  system, which is reported lowest experimental and theoretical results in the thermoelectric system.

#### 4. Outlook and challenge

It is of interest to note that the lowest thermal conductivity is always observed in an amorphous material, since the average

phonon mfp is on the order of the lattice constant ( $\sim 0.2\text{--}0.5 \text{ nm}$ ). The lowest thermal conductivity can be estimated to be  $\kappa \sim 0.25\text{--}1 \text{ W m}^{-1} \text{ K}^{-1}$ , which is confirmed by more sophisticated theories [110]. Recent reports in superlattices of  $\text{WSe}_2/\text{W}$  layers, however, are quite intriguing as they suggested cross-plane lattice thermal conductivity values as low as  $0.02 \text{ W m}^{-1} \text{ K}^{-1}$  [111]. While the mechanism is not fully understood, it is likely that the layering creates large asymmetry in the directional phonon density of states and low coupling between phonons in different directions. Therefore, it is believed that new physical understanding need to be urgently developed to make much lower thermal conductivity become possible.

To reach ZT values of 3 or greater, it seems to be difficult to date. It needs dramatic enhancements in the power factor, which depend on further reduction in the thermal conductivity and increase the electron conductivity. With regards to thermal conductivity, any further reduction below the amorphous limit can only occur if one can actively change the group velocity or reduce the number of phonon modes that propagate. This could result from coherent or correlated scattering effects, but so far this has remained elusive for phonons (although widely known for electrons) and thermal conductivity reduction through such mechanisms has never been conclusively demonstrated. These point to exciting scientific opportunities and create an open challenge to theorists and experimentalists alike to come up with new scattering mechanisms and concepts that will help achieve very large increases in the power factor and simultaneous decreases in thermal conductivity.

Technically, high-performing thermoelectric properties appear to depend sensitively on the nanostructure, synthesis approach and device assembly. Various approaches will continue to study thermoelectric nanomaterials with narrow bandgaps, heavy elements doping, point defects loading and nanostructuring. Especially, for practical thermoelectric applications, the synthetic approaches of thermoelectric nanomaterials, should be: (1) scalable, high-quality and low cost, with tuneable thermoelectric properties, (2) the nanostructured materials must be able to form dense compacts for machining/device integration (device-controllable), (3) the nanostructured material should demonstrate an enhanced ZT over the bulk material and finally (4) the compacted nanoscale features should be with high thermal stability for extended periods of time. Continued research to gain a more quantitative understanding is required to allow the rational design and preparation of optimized nanostructured

**Table 1** Thermoelectric properties of PGEC, low-dimensional and nanostructured materials synthesized by various synthetic methods in the past two decades.

Material systems	Carrier type	ZT	$\kappa_L$ [ $\text{W m}^{-1} \text{K}^{-1}$ ]	$T$	Synthetic method*	Ref.
<b>Skutterudites <math>\text{CoSb}_3</math></b>						
$\text{Yb}_{0.19}\text{Co}_4\text{Sb}_{12}$	n	1	–	600 K	HP	[44]
$\text{In}_{0.25}\text{Co}_4\text{Sb}_{12}$	n	1.2	2	575 K	SSR	[45]
$\text{CoSb}_{2.75}\text{Sn}_{0.05}\text{Te}_{0.20}$	n	1.1	2.04	823 K	MA+SPS	[46]
$\text{Ba}_{0.14}\text{In}_{0.23}\text{Co}_4\text{Sb}_{11.84}$	n	1.34	0.74	850 K	MAG+SPS	[47]
$\text{Yb}_{0.2}\text{Co}_4\text{Sb}_{12.3}$	n	1.26	–	800 K	MAG+SPS	[48]
$\text{Yb}_{0.3}\text{Co}_4\text{Sb}_{12.3}$	n	1.3	–	800 K	MS+SPS	[49]
$\text{Na}_{0.48}\text{Co}_4\text{Sb}_{12}$	–	1.25	–	850 K	MAG+HP	[50]
$\text{Ba}_{0.08}\text{La}_{0.05}\text{Yb}_{0.04}\text{Co}_4\text{Sb}_{12}$	n	1.7	–	850 K	MAG+SPS	[52]
<b>2D Materials: quantum well or superlattices</b>						
$\text{PbTe}/\text{Pb}_{1-x}\text{Eu}_x\text{Te}$	–	2.0	–	RT	MBE	[69]
$\text{PbSeTe}/\text{PbTe}$	n	2.0	0.58	RT	MBE	[15]
$\text{Bi}_2\text{Te}_3/\text{Sb}_2\text{Te}_3$	p	2.4	0.22	300 K	–	[14]
$\text{Bi}_2\text{Te}_3/\text{Bi}_2\text{Te}_{2.83}\text{Se}_{0.17}$	N	1.4	0.58	300 K	–	[14]
<b>Nanowire-based materials</b>						
Si nanowires	–	0.6	1.2	RT	EE	[20]
Si nanowires	p	1	–	200 K	SNAP	[19]
<b><math>\text{Bi}_2\text{Te}_3</math>-based nanocomposites</b>						
$\text{BiSbTe}$	p	1.2	–	RT	HEBM+HP	[21]
$\text{BiSbTe}$	p	1.4	–	373 K	HEBM+HP	[21]
$\text{BiSbTe}$	p	1.3	–	373 K	HEBM+HP	[80]
$\text{BiSbTe}$	p	1.4	–	373 K	HEBM+HP	[81]
$\text{Bi}_2\text{Te}_{2.7}\text{Se}_{0.3}$	n	1.04	–	498 K	HEBM+HP	[82]
$(\text{Bi,Sb})_2\text{Te}_3$	p	1.5	–	390 K	MS+SPS	[83]
$(\text{BiSb})_2\text{Te}_3$	p	1.47	–	440 K	HS+HP	[84]
$\text{Bi}_{0.52}\text{Sb}_{1.48}\text{Te}_3$	p	1.56	0.26	300 K	MS+SPS	[86]
$\text{Bi}_2\text{Te}_3$	n	1	0.3	450 K	HS+HP	[87]
$\text{Bi}_{0.4}\text{Sb}_{1.6}\text{Te}_3$	p	1.5	0.16	RT	MS+HP	[88]
$\text{Bi}_{0.4}\text{Sb}_{1.6}\text{Te}_3$	p	1.8	–	316 K	MS+HP	[88]
<b>PbTe-based nanocomposites</b>						
$\text{AgPb}_{18}\text{SbTe}_{20}$	n	2.2	–	800 K	NP	[16]
$\text{Ag}_{0.5}\text{Pb}_6\text{Sn}_2\text{Sb}_{0.2}\text{Te}_{10}$	p	1.45	0.43	630 K	NP	[90]
$\text{Ag}_{0.53}\text{Pb}_{18}\text{Sb}_{1.2}\text{Te}_{20}$	n	1.7	–	700 K	NP	[91]
$\text{K}_{0.95}\text{Pb}_{20}\text{Sb}_{1.2}\text{Te}_{22}$	n	1.6	0.4	750 K	NP	[92]
$\text{Na}_{0.95}\text{Pb}_{20}\text{SbTe}_{22}$	p	1.7	0.74	700 K	NP	[17]
$\text{PbTe-PbS8\%}$	n	1.4	–	750 K	NP	[93]
$\text{PbTe-Pb-Sb}$	n	1.4	0.6	700 K	NP	[94]
$\text{PbTe-Si}$	n	0.9	–	675 K	NP	[95]
$\text{Pb}_{9.6}\text{Sb}_{0.2}\text{Te}_3\text{Se}_7$	n	1.2	0.4	650 K	NP	[97]
$(\text{Pb}_{0.95}\text{Sn}_{0.05}\text{Te})_{0.92}(\text{PbS})_{0.08}$	n	1.50	0.4	642 K	NP	[23]
2% SrTe-containing PbTe	p	1.7	0.45	800 K	NP	[100]
$\text{NaPb}_{18}\text{BiTe}_{20}$	p	1.3	–	670 K	NP	[103]
$\text{Ag}_{0.8}\text{Pb}_{22.5}\text{SbTe}_{20}$	n	1.5	0.89	700 K	MA+SPS	[106]
<b>SiGe-based nanocomposites</b>						
$\text{Si}_{80}\text{Ge}_{20}$	p	0.95	–	1073 K	HEBM+HP	[107]
$\text{Si}_{80}\text{Ge}_{20}\text{P}_2$	n	1.3	–	1173 K	HEBM+HP	[25]
<b>New thermoelectric materials</b>						
$\text{In}_4\text{Se}_{3-\delta}$	n	1.48	–	705 K	Bridgeman method	[26]
$\text{In}_4\text{Se}_{3-x}\text{Cl}_{0.03}$	n	1.53	–	698 K	Bridgeman method	[109]
$\beta\text{-Cu}_{2-x}\text{Se}$	p	1.5	0.4	1000 K	MAG+SPS	[28]
$\beta\text{-Zn}_4\text{Sb}_3$	p	1.35	–	673 K	Bridgeman method	[22]

\*The abbreviations used in the column of the synthetic method represent the following meanings: SSR=solid state reaction; MA=mechanical alloying; HEBM=high energy ball milling; MAG=melting, annealing and grinding; MS=melt spinning; NP=nanoprecipitation; SS=solvothermal synthesis; HS=hydrothermal synthesis; EE=electroless etching; SNAP=self-assembled nanophase particle; MBE=molecular-beam epitaxy; HP=hot pressing; SPS=spark plasma sintering.

thermoelectric materials and accelerate the wide adoption of thermoelectric technologies in power generation and cooling applications.

### Acknowledgement

This work was supported by the Australian Research Council. Dr Chen thanks QLD government for a smart state future fellowship and a UQ research foundation excellent award.

### References

- G.J. Snyder, E.S. Toberer, Complex thermoelectric materials, *Nature Materials* 7 (2008) 105–114.
- G.S. Nolas, J. Poon, M. Kanatzidis, Recent developments in bulk thermoelectric materials, *MRS Bulletin* 31 (2006) 199–205.
- H. Böttner, G. Chen, R. Venkatasubramanian, Aspects of thin-film superlattice thermoelectric materials, devices, and applications, *MRS Bulletin* 31 (2006) 211–217.
- T.M. Tritt, M.A. Subramanian, Thermoelectric materials, phenomena, and applications: a bird's eye view, *MRS Bulletin* 31 (2006) 188–194.
- L.E. Bell, Cooling, heating, generating power, and recovering waste heat with thermoelectric systems, *Science (New York, NY)* 321 (2008) 1457–1461.
- A.J. Minnich, M.S. Dresselhaus, Z.F. Ren, G. Chen, Bulk nanostructured thermoelectric materials: current research and future prospects, *Energy & Environmental Science* 2 (2009) 466–479.
- Y.C. Lan, A.J. Minnich, G. Chen, Z.F. Ren, Enhancement of thermoelectric figure-of-merit by a bulk nanostructuring approach, *Advanced Functional Materials* 20 (2010) 357–376.
- J. Baxter, Z.X. Bian, G. Chen, D. Danielson, M.S. Dresselhaus, A.G. Fedorov, et al., Nanoscale design to enable the revolution in renewable energy, *Energy & Environmental Science* 2 (2009) 559–588.
- H.J. Goldsmid, R.W. Douglas, The use of semiconductors in thermoelectric refrigeration, *British Journal of Applied Physics* 5 (1954) 386–390.
- H.J. Goldsmid, A.R. Sheard, D.A. Wright, The performance of bismuth telluride thermojunctions, *British Journal of Applied Physics* 9 (1958) 365–370.
- J.P. Dismukes, E. Ekstrom, D.S. Beers, E.F. Steigmeier, I. Kudman, Thermal+electrical properties of heavily doped Ge-Si alloys up to 1300 degrees K, *Journal of Applied Physics* 35 (1964) 2899–2907.
- T.C. Harman, D.L. Spears, M.J. Manfra, High thermoelectric figures of merit in PbTe quantum wells, *Journal of Electronic Materials* 25 (1996) 1121–1127.
- D.Y. Chung, T. Hogan, P. Brazis, M. Rocci-Lane, C. Kannerwulf, M. Bastea, et al., CsBi<sub>4</sub>Te<sub>6</sub>: a high-performance thermoelectric material for low-temperature applications, *Science (New York, NY)* 287 (2000) 1024–1027.
- R. Venkatasubramanian, E. Siivola, T. Colpitts, B. O'Quinn, Thin-film thermoelectric devices with high room-temperature figures of merit, *Nature* 413 (2001) 597–602.
- T.C. Harman, P.J. Taylor, M.P. Walsh, B.E. LaForge, Quantum dot superlattice thermoelectric materials and devices, *Science (New York, NY)* 297 (2002) 2229–2232.
- K.F. Hsu, S. Loo, F. Guo, W. Chen, J.S. Dyck, C. Uher, et al., Cubic AgPb<sub>m</sub>SbTe<sub>2+m</sub>: bulk thermoelectric materials with high figure of merit, *Science (New York, NY)* 303 (2004) 818–821.
- P.F.R. Poudeu, J. D'Angelo, A.D. Downey, J.L. Short, T.P. Hogan, M.G. Kanatzidis, High thermoelectric figure of merit and nanostructuring in bulk p-type Na<sub>1-x</sub>Pb<sub>m</sub>Sb<sub>y</sub>Te<sub>m+2</sub>, *Angewandte Chemie, International Edition* 45 (2006) 3835–3839.
- A. Saramat, G. Svensson, A.E.C. Palmqvist, C. Stiewe, E. Mueller, D. Platzek, et al., Large thermoelectric figure of merit at high temperature in Czochralski-grown clathrate Ba<sub>8</sub>Ga<sub>16</sub>Ge<sub>30</sub>, *Journal of Applied Physics* 99 (2006) 023708.
- A.I. Boukai, Y. Bunimovich, J. Tahir-Kheli, J.-K. Yu, W.A. Goddard III, J.R. Heath, Silicon nanowires as efficient thermoelectric materials, *Nature* 451 (2008) 168–171.
- A.I. Hochbaum, R. Chen, R.D. Delgado, W. Liang, E.C. Garnett, M. Najarian, et al., Enhanced thermoelectric performance of rough silicon nanowires, *Nature* 451 (2008) 163–U165.
- B. Poudel, Q. Hao, Y. Ma, Y. Lan, A. Minnich, B. Yu, et al., High-thermoelectric performance of nanostructured bismuth antimony telluride bulk alloys, *Science (New York, NY)* 320 (2008) 634–638.
- G.J. Snyder, M. Christensen, E. Nishibori, T. Caillat, B.B. Iversen, Disordered zinc in Zn<sub>4</sub>Sb<sub>3</sub> with phonon-glass and electron-crystal thermoelectric properties, *Nature Materials* 3 (2004) 458–463.
- J. Androulakis, C.H. Lin, H.J. Kong, C. Uher, C.I. Wu, T. Hogan, et al., Spinodal decomposition and nucleation and growth as a means to bulk nanostructured thermoelectrics: enhanced performance in Pb<sub>1-x</sub>Sn<sub>x</sub>Te–PbS, *Journal of the American Chemical Society* 129 (2007) 9780–9788.
- J.P. Heremans, V. Jovovic, E.S. Toberer, A. Saramat, K. Kurosaki, A. Charoenphakdee, et al., Enhancement of thermoelectric efficiency in PbTe by distortion of the electronic density of states, *Science (New York, NY)* 321 (2008) 554–557.
- X.W. Wang, H. Lee, Y.C. Lan, G.H. Zhu, G. Joshi, D.Z. Wang, et al., Enhanced thermoelectric figure of merit in nanostructured n-type silicon germanium bulk alloy, *Applied Physics Letters* 93 (2008) 193121.
- J.S. Rhyee, K.H. Lee, S.M. Lee, E. Cho, S.I. Kim, E. Lee, et al., Peierls distortion as a route to high thermoelectric performance in In<sub>4</sub>Se<sub>3-δ</sub> crystals, *Nature* 459 (2009) 965–968.
- Y. Pei, X. Shi, A. LaLonde, H. Wang, L. Chen, G.J. Snyder, Convergence of electronic bands for high performance bulk thermoelectrics, *Nature* 473 (2011) 66–69.
- H. Liu, X. Shi, F. Xu, L. Zhang, W. Zhang, L. Chen, et al., Copper ion liquid-like thermoelectrics, *Nature Materials* 11 (2012) 422–425.
- T.M. Tritt, H. Böttner, L. Chen, Thermoelectrics: direct solar thermal energy conversion, *MRS Bulletin* 33 (2008) 366–368.
- J.R. Sootsman, D.Y. Chung, M.G. Kanatzidis, New and old concepts in thermoelectric materials, *Angewandte Chemie, International Edition* 48 (2009) 8616–8639.
- C.J. Vineis, A. Shakouri, A. Majumdar, M.G. Kanatzidis, Nanostructured thermoelectrics: big efficiency gains from small features, *Advanced Materials* 22 (2010) 3970–3980.
- P. Vaquero, A.V. Powell, Recent developments in nanostructured materials for high-performance thermoelectrics, *Journal of Materials Chemistry* 20 (2010) 9577–9584.
- S.K. Bux, J.P. Fleurial, R.B. Kaner, Nanostructured materials for thermoelectric applications, *Chemical Communications* 46 (2010) 8311–8324.
- M.G. Kanatzidis, Nanostructured thermoelectrics: the new paradigm?, *Chemistry of Materials* 22 (2009) 648–659.
- D.L. Medlin, G.J. Snyder, Interfaces in bulk thermoelectric materials: a review for current opinion in colloid and interface science, *Current Opinion in Colloid & Interface Science* 14 (2009) 226–235.
- P. Pichanusakorn, P. Bandaru, Nanostructured thermoelectrics, *Materials Science and Engineering: R: Reports* 67 (2010) 19–63.
- M. Zebarjadi, K. Esfarjani, M.S. Dresselhaus, Z.F. Ren, G. Chen, Perspectives on thermoelectrics: from fundamentals to device applications, *Energy & Environmental Science* 5 (2012) 5147–5162.
- C. Wood, *Materials for thermoelectric energy-conversion*, *Reports on Progress in Physics* 51 (1988) 459–539.
- G.A. Slack, in: M. Rowe (Ed.), *CRC Handbook of Thermoelectrics*, CRC Press, Boca Raton, FL, 1995.



- [40] J.R. Szczech, J.M. Higgins, S. Jin, Enhancement of the thermoelectric properties in nanoscale and nanostructured materials, *Journal of Materials Chemistry* 21 (2011) 4037–4055.
- [41] M.S. Dresselhaus, G. Chen, M.Y. Tang, R.G. Yang, H. Lee, D.Z. Wang, et al., New directions for low-dimensional thermoelectric materials, *Advanced Materials* 19 (2007) 1043–1053.
- [42] B.C. Sales, D. Mandrus, B.C. Chakoumakos, V. Keppens, J.R. Thompson, Filled skutterudite antimonides: Electron crystals and phonon glasses, *Physical Review B* 56 (1997) 15081.
- [43] B.C. Sales, D. Mandrus, R.K. Williams, Filled skutterudite antimonides: a new class of thermoelectric materials, *Science* (New York, NY) 272 (1996) 1325–1328.
- [44] G.S. Nolas, M. Kaeser, R.T. Littleton, T.M. Tritt, High figure of merit in partially filled ytterbium skutterudite materials, *Applied Physics Letters* 77 (2000) 1855–1857.
- [45] T. He, J. Chen, H.D. Rosenfeld, M.A. Subramanian, Thermoelectric properties of indium-filled skutterudites, *Chemistry of Materials* 18 (2006) 759–762.
- [46] W.S. Liu, B.P. Zhang, L.D. Zhao, J.F. Li, Improvement of thermoelectric performance of  $\text{CoSb}_{(3-x)}\text{Te}_{(x)}$  skutterudite compounds by additional substitution of IVB-group elements for Sb, *Chemistry of Materials* 20 (2008) 7526–7531.
- [47] W. Zhao, P. Wei, Q. Zhang, C. Dong, L. Liu, X. Tang, Enhanced thermoelectric performance in barium and indium double-filled skutterudite bulk materials via orbital hybridization induced by indium filler, *Journal of the American Chemical Society* 131 (2009) 3713–3720.
- [48] H. Li, X.F. Tang, X.L. Su, Q.J. Zhang, Preparation and thermoelectric properties of high-performance Sb additional  $\text{Yb}_{(0.2)}\text{Co}_{(4)}\text{Sb}_{(12+y)}$  bulk materials with nanostructure, *Applied Physics Letters* 92 (2008) 202114.
- [49] H. Li, X.F. Tang, Q.J. Zhang, C. Uher, Rapid preparation method of bulk nanostructured  $\text{Yb}_{(0.3)}\text{Co}_{(4)}\text{Sb}_{(12+y)}$  compounds and their improved thermoelectric performance, *Applied Physics Letters* 93 (2008) 202114.
- [50] Y.Z. Pei, J. Yang, L.D. Chen, W. Zhang, J.R. Salvador, J.H. Yang, Improving thermoelectric performance of caged compounds through light-element filling, *Applied Physics Letters* 95 (2009) 042101.
- [51] J.L. Mi, T.J. Zhu, X.B. Zhao, J. Ma, Nanostructuring and thermoelectric properties of bulk skutterudite compound  $\text{CoSb}_3$ , *Journal of Applied Physics* 101 (2007) 054314.
- [52] X. Shi, J. Yang, J.R. Salvador, M. Chi, J.Y. Cho, H. Wang, et al., Multiple-filled skutterudites: High thermoelectric figure of merit through separately optimizing electrical and thermal transports, *Journal of the American Chemical Society* 133 (2011) 7837–7846.
- [53] X. Shi, J. Yang, S. Bai, J. Yang, H. Wang, M. Chi, et al., On the design of high-efficiency thermoelectric clathrates through a systematic cross-substitution of framework elements, *Advanced Functional Materials* 20 (2010) 755–763.
- [54] Y. Liu, L.M. Wu, L.H. Li, S.W. Du, J.D. Corbett, L. Chen, The antimony-based type I clathrate compounds  $\text{Cs}_8\text{Cd}_{(18)}\text{Sb}_{(28)}$  and  $\text{Cs}_8\text{Zn}_{(18)}\text{Sb}_{(28)}$ , *Angewandte Chemie, International Edition* 48 (2009) 5305–5308.
- [55] C.L. Condon, S.M. Kauzlarich, F. Gascoin, G.J. Snyder, Thermoelectric properties and microstructure of  $\text{Ba}_8\text{Al}_4\text{Si}_{31}$  and  $\text{EuBa}_7\text{Al}_{13}\text{Si}_{33}$ , *Chemistry of Materials* 18 (2006) 4939–4945.
- [56] H. Kleinke, New bulk materials for thermoelectric power generation: clathrates and complex antimonides, *Chemistry of Materials* 22 (2010) 604–611.
- [57] M. Christensen, B.B. Iversen, Host structure engineering in thermoelectric clathrates, *Chemistry of Materials* 19 (2007) 4896–4905.
- [58] M. Christensen, S. Johnsen, M. Sondergaard, J. Overgaard, H. Birkedal, B.B. Iversen, Fast preparation and characterization of quaternary thermoelectric clathrates, *Chemistry of Materials* 21 (2009) 122–127.
- [59] M. Christensen, N. Lock, J. Overgaard, B.B. Iversen, Crystal structures of thermoelectric n- and p-type  $\text{Ba}_8\text{Ga}_{16}\text{Ge}_{30}$  studied by single crystal, multitemperature, neutron diffraction, conventional X-ray diffraction and resonant synchrotron X-ray diffraction, *Journal of the American Chemical Society* 128 (2006) 15657–15665.
- [60] M. Christensen, S. Johnsen, B.B. Iversen, Thermoelectric clathrates of type I, *Dalton Transactions* 39 (2010) 978–992.
- [61] L.T.K. Nguyen, U. Aydemir, M. Baitinger, E. Bauer, H. Borrmann, U. Burkhardt, et al., Atomic ordering and thermoelectric properties of the n-type clathrate  $\text{Ba}_{(8)}\text{Ni}_{(3.5)}\text{Ge}_{(42.1)}\text{square}_{(0.4)}$ , *Dalton Transactions* 39 (2010) 1071–1077.
- [62] U. Aydemir, C. Candolfi, H. Borrmann, M. Baitinger, A. Ormeci, W. Carrillo-Cabrera, et al., Crystal structure and transport properties of  $\text{Ba}_{(8)}\text{Ge}_{(43)}\text{square}_{(3)}$ , *Dalton Transactions* 39 (2010) 1078–1088.
- [63] G.J. Snyder, E.S. Toberer, Complex thermoelectric materials, *Nature Materials* 7 (2008) 105–114.
- [64] B.B. Iversen, Fulfilling thermoelectric promises: beta- $\text{Zn}_4\text{Sb}_3$  from materials research to power generation, *Journal of Materials Chemistry* 20 (2010) 10778–10787.
- [65] L.D. Hicks, M.S. Dresselhaus, Effect of quantum-well structures on the thermoelectric figure of merit, *Physical Review B* 47 (1993) 12727.
- [66] L.D. Hicks, T.C. Harman, M.S. Dresselhaus, Use of quantum-well superlattices to obtain a high figure of merit from nonconventional thermoelectric materials, *Applied Physics Letters* 63 (1993) 3230–3232.
- [67] I. Chowdhury, R. Prasher, K. Lofgreen, G. Chrysler, S. Narasimhan, R. Mahajan, et al., On-chip cooling by superlattice-based thin-film thermoelectrics, *Nature Nanotechnology* 4 (2009) 235–238.
- [68] J.J. Urban, D.V. Talapin, E.V. Shevchenko, C.R. Kagan, C.B. Murray, Synergism in binary nanocrystal superlattices leads to enhanced p-type conductivity in self-assembled  $\text{PbTe}/\text{Ag}_{-2}\text{Te}$  thin films, *Nature Materials* 6 (2007) 115–121.
- [69] L.D. Hicks, T.C. Harman, X. Sun, M.S. Dresselhaus, Experimental study of the effect of quantum-well structures on the thermoelectric figure of merit, *Physical Review B* 53 (1996) R10493.
- [70] E.I. Rogacheva, O.N. Nashchekina, A.V. Meriuts, S.G. Lyubchenko, M.S. Dresselhaus, G. Dresselhaus, Quantum size effects in n-PbTe/p-SnTe/n-PbTe heterostructures, *Applied Physics Letters* 86 (2005) 063103.
- [71] A. Shakouri, Thermoelectric, thermionic and thermophotovoltaic energy conversion, *Proceedings of the International Conference on Thermoelectrics* (2005) 492–497.
- [72] L.D. Hicks, M.S. Dresselhaus, Thermoelectric figure of merit of a one-dimensional conductor, *Physical Review B* 47 (1993) 16631–16634.
- [73] X.B. Zhao, X.H. Ji, Y.H. Zhang, T.J. Zhu, J.P. Tu, X.B. Zhang, Bismuth telluride nanotubes and the effects on the thermoelectric properties of nanotube-containing nanocomposites, *Applied Physics Letters* 86 (2005) 062111.
- [74] G. Zhang, Q. Yu, W. Wang, X. Li, Nanostructures for thermoelectric applications: synthesis, growth mechanism, and property studies, *Advanced Materials* 22 (2010) 1959–1962.
- [75] A.I. Persson, Y.K. Koh, D.G. Cahill, L. Samuelson, H. Linke, Thermal conductance of InAs nanowire composites, *Nano Letters* 9 (2009) 4484–4488.
- [76] A. Mavrokefalos, A.L. Moore, M.T. Pettes, L. Shi, W. Wang, X. Li, Thermoelectric and structural characterizations of individual electrodeposited bismuth telluride nanowires, *Journal of Applied Physics* 105 (2009) 104318.
- [77] F. Zhou, J.H. Seol, A.L. Moore, L. Shi, Q.L. Ye, R. Scheffler, One-dimensional electron transport and thermopower in an individual InSb nanowire, *Journal of Physics: Condensed Matter* 18 (2006) 9651–9657.
- [78] F. Zhou, A.L. Moore, M.T. Pettes, Y. Lee, J.H. Seol, Q.L. Ye, et al., Effect of growth base pressure on the thermoelectric properties

- of indium antimonide nanowires, *Journal of Physics D: Applied Physics* 43 (2010) 025406.
- [79] P. Kim, L. Shi, A. Majumdar, P.L. McEuen, Mesoscopic thermal transport and energy dissipation in carbon nanotubes, *Physica B: Condensed Matter* 323 (2002) 67–70.
- [80] Y. Ma, Q. Hao, B. Poudel, Y. Lan, B. Yu, D. Wang, et al., Enhanced thermoelectric figure-of-merit in p-type nanostructured bismuth antimony tellurium alloys made from elemental chunks, *Nano Letters* 8 (2008) 2580–2584.
- [81] Y. Lan, B. Poudel, Y. Ma, D. Wang, M.S. Dresselhaus, G. Chen, et al., Structure study of bulk nanograined thermoelectric bismuth antimony telluride, *Nano Letters* 9 (2009) 1419–1422.
- [82] X. Yan, B. Poudel, Y. Ma, W.S. Liu, G. Joshi, H. Wang, et al., Experimental studies on anisotropic thermoelectric properties and structures of n-Type  $\text{Bi}_{(2)}\text{Te}_{(2.7)}\text{Se}_{(0.3)}$ , *Nano Letters* 10 (2010) 3373–3378.
- [83] W. Xie, J. He, H.J. Kang, X. Tang, S. Zhu, M. Laver, et al., Identifying the specific nanostructures responsible for the high thermoelectric performance of  $(\text{Bi,Sb})_2\text{Te}_3$  nanocomposites, *Nano Letters* 10 (2010) 3283–3289.
- [84] Y.Q. Cao, X.B. Zhao, T.J. Zhu, X.B. Zhang, J.P. Tu, Syntheses and thermoelectric properties of  $\text{Bi}_{(2)}\text{Te}_{(3)}/\text{Sb}_{(2)}\text{Te}_{(3)}$  bulk nanocomposites with laminated nanostructure, *Applied Physics Letters* 92 (2008) 143106.
- [85] W. Xie, X. Tang, Y. Yan, Q. Zhang, T.M. Tritt, High thermoelectric performance  $\text{BiSbTe}$  alloy with unique low-dimensional structure, *Journal of Applied Physics* 105 (2009) 113713.
- [86] W. Xie, X. Tang, Y. Yan, Q. Zhang, T.M. Tritt, Unique nanostructures and enhanced thermoelectric performance of melt-spun  $\text{BiSbTe}$  alloys, *Applied Physics Letters* 94 (2009) 102111.
- [87] X.B. Zhao, S.H. Yang, Y.Q. Cao, J.L. Mi, Q. Zhang, T.J. Zhu, Synthesis of nanocomposites with improved thermoelectric properties, *Journal of Electronic Materials* 38 (2009) 1017–1024.
- [88] S. Fan, J. Zhao, J. Guo, Q. Yan, J. Ma, H.H. Hng, p-type  $\text{Bi}_{(0.4)}\text{Sb}_{(1.6)}\text{Te}_{(3)}$  nanocomposites with enhanced figure of merit, *Applied Physics Letters* 96 (2010) 182104.
- [89] X.A. Fan, J.Y. Yang, Z. Xie, K. Li, W. Zhu, X.K. Duan, et al.,  $\text{Bi}_2\text{Te}_3$  hexagonal nanoplates and thermoelectric properties of n-type  $\text{Bi}_2\text{Te}_3$  nanocomposites, *Journal of Physics D: Applied Physics* 40 (2007) 5975–5979.
- [90] J. Androulakis, K.F. Hsu, R. Pcionek, H. Kong, C. Uher, J.J. Dangelo, et al., Nanostructuring and high thermoelectric efficiency in p-type  $\text{Ag}(\text{Pb}_{1-y}\text{Sn}_y)(\text{m})\text{SbTe}_{2+m}$ , *Advanced Materials* 18 (2006) 1170–1173.
- [91] B.A. Cook, M.J. Kramer, J.L. Harringa, M.K. Han, D.Y. Chung, M.G. Kanatzidis, Analysis of nanostructuring in high figure-of-merit  $\text{Ag}_{(1-x)}\text{Pb}_{(m)}\text{SbTe}_{(2+m)}$  thermoelectric materials, *Advanced Functional Materials* 19 (2009) 1254–1259.
- [92] P.F.P. Poudeu, A. Gueguen, C.-I. Wu, T. Hogan, M.G. Kanatzidis, High figure of merit in nanostructured n-type  $\text{KPb}_{(m)}\text{SbTe}_{(m+2)}$  thermoelectric materials, *Chemistry of Materials* 22 (2010) 1046–1053.
- [93] S.N. Girard, J. He, C. Li, S. Moses, G. Wang, C. Uher, et al., In situ nanostructure generation and evolution within a bulk thermoelectric material to reduce lattice thermal conductivity, *Nano Letters* 10 (2010) 2825–2831.
- [94] J.R. Sootsman, H. Kong, C. Uher, J.J. D'Angelo, C.-I. Wu, T.P. Hogan, et al., Large enhancements in the thermoelectric power factor of bulk  $\text{PbTe}$  at high temperature by synergistic nanostructuring, *Angewandte Chemie, International Edition* 47 (2008) 8618–8622.
- [95] J.R. Sootsman, J. He, V.P. Dravid, S. Ballikaya, D. Vermeulen, C. Uher, et al., Microstructure and thermoelectric properties of mechanically robust  $\text{PbTe-Si}$  eutectic composites, *Chemistry of Materials* 22 (2010) 869–875.
- [96] J. He, S.N. Girard, M.G. Kanatzidis, V.P. Dravid, Microstructure-lattice thermal conductivity correlation in nanostructured  $\text{PbTe}_{(0.7)}\text{S}_{(0.3)}$  thermoelectric materials, *Advanced Functional Materials* 20 (2010) 764–772.
- [97] P.F.P. Poudeu, J. D'Angelo, H. Kong, A. Downey, J.L. Short, R. Pcionek, et al., Nanostructures versus solid solutions: low lattice thermal conductivity and enhanced thermoelectric figure of merit in  $\text{Pb}_{9.6}\text{Sb}_{0.2}\text{Te}_{10-x}\text{Se}_x$  bulk materials, *Journal of the American Chemical Society* 128 (2006) 14347–14355.
- [98] E. Quarez, K.F. Hsu, R. Pcionek, N. Frangis, E.K. Polychroniadis, M.G. Kanatzidis, Nanostructuring, compositional fluctuations, and atomic ordering in the thermoelectric materials  $\text{AgPb}_m\text{SbTe}_{2+m}$ . The myth of solid solutions, *Journal of the American Chemical Society* 127 (2005) 9177–9190.
- [99] J. He, J.R. Sootsman, S.N. Girard, J.C. Zheng, J. Wen, Y. Zhu, et al., On the origin of increased phonon scattering in nanostructured  $\text{PbTe}$  based thermoelectric materials, *Journal of the American Chemical Society* 132 (2010) 8669–8675.
- [100] K. Biswas, J. He, Q. Zhang, G. Wang, C. Uher, V.P. Dravid, et al., Strained endotaxial nanostructures with high thermoelectric figure of merit, *Nature Chemistry* 3 (2011) 160–166.
- [101] J.R. Sootsman, R.J. Pcionek, H. Kong, C. Uher, M.G. Kanatzidis, Strong reduction of thermal conductivity in nanostructured  $\text{PbTe}$  prepared by matrix encapsulation, *Chemistry of Materials* 18 (2006) 4993–4995.
- [102] M.-K. Han, K. Hoang, H. Kong, R. Pcionek, C. Uher, K.M. Paraskevopoulos, et al., Substitution of Bi for Sb and its role in the thermoelectric properties and nanostructuring in  $\text{Ag}_{1-x}\text{Pb}_{18M}\text{Te}_{20}$  ( $M=\text{Bi, Sb}$ ) ( $x=0, 0.14, 0.3$ ), *Chemistry of Materials* 20 (2008) 3512–3520.
- [103] A. Gueguen, P.F.P. Poudeu, C.-P. Li, S. Moses, C. Uher, J. He, et al., Thermoelectric properties and nanostructuring in the p-type materials  $\text{NaPb}_{18-x}\text{Sn}_x\text{MTe}_{20}$  ( $M=\text{Sb, Bi}$ ), *Chemistry of Materials* 21 (2009) 1683–1694.
- [104] K. Ahn, C.-P. Li, C. Uher, M.G. Kanatzidis, Thermoelectric properties of the compounds  $\text{AgPb}_m\text{LaTe}_{m+2}$ , *Chemistry of Materials* 22 (2009) 876–882.
- [105] C.B. Lioutas, N. Frangis, I. Todorov, D.Y. Chung, M.G. Kanatzidis, Understanding nanostructures in thermoelectric materials: an electron microscopy study of  $\text{AgPb}_{18}\text{SbSe}_{20}$  crystals, *Chemistry of Materials* 22 (2010) 5630–5635.
- [106] M. Zhou, J. Li, T. Kita, Nanostructured  $\text{AgPb}_m\text{SbTe}_{m+2}$  system bulk materials with enhanced thermoelectric performance, *Journal of the American Chemical Society* 130 (2008) 4527–4532.
- [107] G. Joshi, H. Lee, Y. Lan, X. Wang, G. Zhu, D. Wang et al., Enhanced thermoelectric figure-of-merit in nanostructured p-type silicon germanium bulk alloys, *Nano Letters* 8 (2008) 4670–4674.
- [108] C.B. Vining, W. Laskow, J.O. Hanson, R.R. Vanderbeck, P.D. Gorsuch, Thermoelectric properties of pressure-sintered  $\text{Si}_{0.8}\text{Ge}_{0.2}$  thermoelectric alloys, *Journal of Applied Physics* 69 (1991) 4333–4340.
- [109] J.S. Rhyee, K. Ahn, K.H. Lee, H.S. Ji, J.-H. Shim, Enhancement of the thermoelectric figure-of-merit in a wide temperature range in  $\text{In}_4\text{Se}_{3-x}\text{Cl}_{0.03}$  bulk crystals, *Advanced Materials* 23 (2011) 2191–2194.
- [110] D.G. Cahill, S.K. Watson, R.O. Pohl, Lower limit to the thermal-conductivity of disordered crystals, *Physical Review B* 46 (1992) 6131–6140.
- [111] C. Chiritescu, D.G. Cahill, N. Nguyen, D. Johnson, A. Bodapati, P. Keblinski, et al., Ultralow thermal conductivity in disordered, layered  $\text{WSe}_2$  crystals, *Science (New York, NY)* 315 (2007) 351–353.



**Professor Jin Zou** received his Ph.D. in Materials Physics from the University of Sydney and worked there for 10 years as a researcher. He is now a Chair in Nanoscience at the University of Queensland. His research interests focus on the nanocharacterization of various semiconductor and functional nanostructures; and he published about 400 journal publications in this field.



**Dr. Zhigang Chen** received his Ph.D. in Material Sciences and Engineering from the Institute of Metal Research (IMR), Chinese Academy of Science (CAS), China, in 2008. He is currently a Queensland Smart Future Fellow at the University of Queensland. In recent years, his research concentrates in developing advanced functional semiconductor nanomaterials for energy-related applications. Dr. Chen has published more than 70 peer reviewed journal articles with over 1700 citations and a H index of 25. He was honoured with the prestigious ARC APD Fellowship, Queensland Smart Future Fellowship, Queensland international Fellowship and UQ Foundation Research Excellent Award.